Available online at www.sciencedirect.com
SCIENCE DIRECT
Journal of Solid State Chemistry 179 (2006) 1775–1781
JOURNAL OF SOLID STATE CHEMISTRY
www.elsevier.com/locate/jssc

The Jahn–Teller distortion and cation ordering in the perovskite Sr_2MnSbO_6

Melina Cheah, Paul J. Saines, Brendan J. Kennedy*

Centre for Structural Biology and Structural Chemistry, School of Chemistry, The University of Sydney, Sydney, NSW 2006, Australia

Received 7 October 2005; received in revised form 2 February 2006; accepted 16 March 2006
Available online 19 April 2006

Abstract

The perovskite Sr_2MnSbO_6 has been synthesized using conventional ceramic techniques and structurally characterized using high-resolution powder X-ray and neutron diffraction. The structure is tetragonal in space group $I4/m$. The octahedra were found to feature Jahn–Teller (JT) distortion due to the presence of Mn^{3+}, and this is identified as strongly contributing to the octahedral tilting. Evidence for *B*-site cation ordering is presented however there is extensive anti-site disorder. The disordering of the Mn^{3+} and Sb^{5+} cations is believed to be a result of the similar size of these two cations and the polarizability of the Sb^{5+} cation. The structure was found to undergo a transition to cubic symmetry at 521 °C with removal of the octahedral tilting leading to the quenching of the JT distortion. This phase transition was found to be continuous and tricritical in nature.

Keywords: Ordered perovskite; Jahn-Tellar distortion; Phase transition

1. Introduction

The favorable structural, electronic and magnetic properties of perovskite-type ABO_3 oxides are often fine-tuned by doping either the *A*- or *B*-type cations. The vast numbers of perovskite-type oxides reported to date are often considered to be testament to the supposed flexibility of the structure. In reality the perovskite structure is very exacting; with the three atoms all on general positions, there is only one variable parameter, the length of the primitive cubic cell [1,2]. The vast majority of materials described as perovskites, like the mineral perovskite ($CaTiO_3$) itself, do not have the cubic aristotype structure. Rather, as a result of co-operative tilting of the BO_6 octahedra, displacement of the cation within the octahedra or ordering of the cations, have one of numerous hetterotype structures [1]. Understanding the complex relationships between composition, structure and properties in perovskites remains a significant challenge in materials chemistry.

Almost 40 years after the unusual magnetic properties of manganese perovskites were first reported, the discovery of the colossal magnetoresistance (CMR) effect in doped manganese perovskites based on $LaMnO_3$ lead to a resurgence of interest in these materials [3]. Analogous CMR properties have been observed in some cation ordered double perovskites based on Sr_2FeMoO_6 [4,5]. A particularly vexing question has been the importance of the Jahn–Teller (JT) effect in these Mn^{3+} (d^4) oxides, and how this effect influences the orbital ordering, structure and properties of doped oxides. It has been suggested that the combination of charge and orbital ordering in the doped-$LaMnO_3$-type materials is an important feature for their CMR behavior [6].

The present paper describes new results for Sr_2MnSbO_6 which is expected to display orbital ordering of the Mn^{3+} cations. That Sr_2MnSbO_6 is tetragonal at room temperature is beyond dispute and this is rationalized in terms of the tolerance factor, t given by $t = r_A + r_O/\sqrt{2}(r_B + r_O)$ where r_A is the ionic radius of the *A*-cation, r_O the radius of oxygen and r_B the weighted average of the ionic radii of the two *B*-site cations. In the case of Sr_2MnSbO_6 the value of the tolerance factor is slightly less than unity [2,7].

*Corresponding author. Fax: +61 2 9351 3329.
E-mail address: kennedyb@chem.usyd.edu.au (B.J. Kennedy).

0022-4596/$ - see front matter © 2006 Elsevier Inc. All rights reserved.
doi:10.1016/j.jssc.2006.03.013

Although the JT effect is expected to result in a tetragonal distortion of the MnO_6 octahedra, by analogy with Sr_2CuWO_6, Sr_2CuTeO_6 and $PrAlO_3$ it appears that the JT-induced distortion can be accommodated within the same tilt system observed for non-JT cations [8–10]. Indeed tilting of the octahedra can induce a tetragonal distortion of the octahedra in the absence of any electronic effects [11]. The results for Sr_2CuWO_6 are important in the present context since these demonstrate that JT distortion, tilting and cation ordering can co-exist.

Ordering of the Mn^{3+} and Sb^{5+} cations in Sr_2MnSbO_6 is less well established [7]. The ionic radii of Mn^{3+} and Sb^{5+} are similar, 0.79 and 0.74 Å [12], and ordering of these cations, should it occur, must be driven primarily by the charge, rather than size, difference. Blasse [13] initially described the Mn^{3+} and Sb^{5+} in Sr_2MnSbO_6 as being disordered whereas Abrahams [14] suggested ordering was present. Both these studies relied on laboratory powder X-ray data that suffers from both poor peak resolution and lack of sensitivity to the precise position of the oxygen atoms. Lufaso et al. [7] attempted to resolve this issue using medium resolution neutron diffraction methods; whilst such data clearly provides greater sensitivity to the oxygen positions it is less sensitive to cation ordering. Lufaso et al. [7] concluded that whilst tilting of the octahedra was present there was no cation ordering. Interestingly they found the JT distortion in Sr_2MnSbO_6 to be smaller than seen across the $LnMnO_3$ perovskite series, suggesting that the disorder of the Mn^{3+} and Sb^{5+} on the one site somehow inhibits, or partially quenches, the JT effect at room temperature. We propose that such quenching should be strongly temperature dependent and that heating the sample should totally remove the distortion.

The objective of the current paper is to present the results of a variable temperature synchrotron X-ray diffraction study on Sr_2MnSbO_6. These results are supplemented by some high-resolution neutron diffraction measurements. These measurements show there is partial ordering of the Mn^{3+} and Sb^{5+} cations and that a continuous tetragonal to cubic transition occurs near 521 °C.

2. Experimental

The sample of Sr_2MnSbO_6 was prepared using conventional solid-state methods from a mixture of $SrCO_3$, MnO_2 and Sb_2O_3. The oxides were finely ground and subsequently heated at 850 °C in air for 48 h and then at 1100 °C for 6 days with periodic regrinding. The sample was then slowly cooled to around 700 °C in the furnace and quenched to room temperature.

The sample purity was established by powder X-ray diffraction measurements using Cu$K\alpha$ radiation on a Shimadzu X-6000 Diffractometer. Synchrotron X-ray powder diffraction patterns were collected on the Debye Scherrer diffractometer at beamline 20B, the Australian National Beamline Facility, at the Photon Factory, Japan [15]. The sample was finely ground and loaded into a 0.3-mm quartz capillary that was rotated during the measurements. Measurements were performed under vacuum to minimize air scattering. Data were recorded using two Fuji image plates. Each image plate is 20×40 cm and covers 40° in 2θ. The data were collected at a wavelength of 0.80282 Å (calibrated using NIST Si 640c standard) over the 2θ range of 5–85° with step size of 0.01°. High temperature measurements were recorded in the same manner using a custom built furnace. Additional high-resolution data were collected at the Advanced Photon Source using 1-BM. These diffraction patterns were collected at a wavelength of 0.61914 Å using a flat plate geometry, a Si(111) double crystal sagitally focusing monochromator, a Si(111) analyzer crystal, and an Oxford cyberstar detector.

Neutron powder diffraction data were collected at the HIFAR facility operated by the Australian Nuclear Science and Technology Organization (ANSTO) using the high-resolution powder diffractometer at a wavelength of 1.371 Å [16]. The sample was held in an aluminum capped vanadium sample holder for the room temperature measurements, which was rotated throughout the measurements, and a stainless steel can for the variable temperature measurements. The diffractometer is equipped with 24 ^{3}He detectors individually separated by 5°. The patterns were collected over the 2θ range 0–150° with step size of 0.05°.

Refinements of appropriate structural models against the powder X-ray and neutron diffraction data obtained during this study were carried out using the computer program Rietica using a pseudo-Voigt peak shape and applying Howard asymmetry correction where required [17].

3. Results and discussion

The synchrotron X-ray diffraction pattern (Fig. 1), was indexed to a tetragonal structure with $a = 5.5391(3)$ Å $\approx \sqrt{2}a_p$ and $c = 8.0951(5)$ Å $\approx 2a_p$, where a_p is the cell parameter of the equivalent primitive cubic cell. The expansion in the cell can arise from tilting of the octahedra and/or ordering of the Mn^{3+} and Sb^{5+} cations [18]. Careful examination of the diffraction pattern shows a broad weak reflection near $2\theta = 7.75°$ ($d = 4.57$ Å at $\lambda = 0.61914$ Å) that is indexed as 1 0 1 on this expanded cell. The observation of this reflection demonstrates that cation ordering occurs. During the analysis of this pattern it was apparent that the 0 0 l reflections were systematically broadened and such anisotropic broadening was included in the refinements. There is evidence for some residual intensity between some Bragg reflections, most obviously between the 0 0 2 and 1 1 0 reflections near $2\theta \sim 9°$ in Fig. 2. This is believed to be a consequence of domain wall broadening. Such broadening effects are often observed in systems near a ferroelastic phase transition [19]. The neutron diffraction pattern (Fig. 2), also shows a broad and very weak 1 0 1 reflection near 17.24° at $\lambda = 1.371$ Å. In addition to this reflection the neutron pattern also showed a number of $h\,k\,l$ reflections indicative of tilting of the

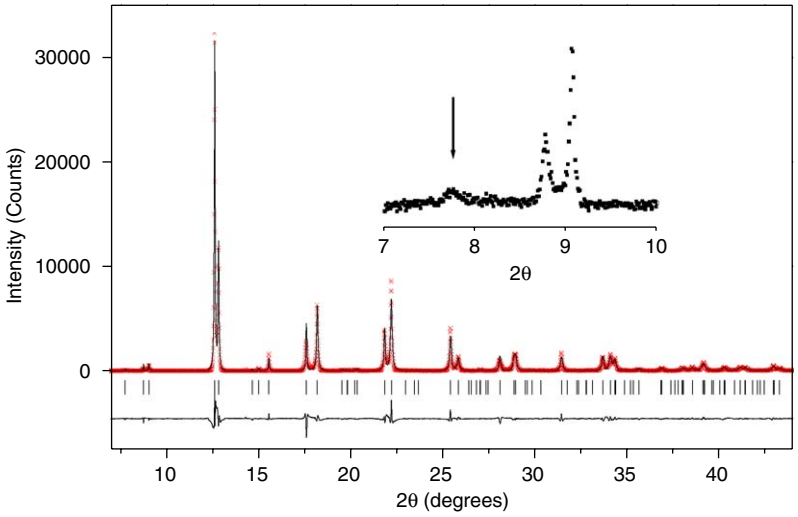

Fig. 1. Observed and calculated synchrotron X-ray profiles for the Rietveld refinement of Sr_2MnSbO_6. The bottom curve is the difference plot on the same intensity scale and the vertical markers show the positions of the space group allowed reflections. The inset shows the broad weak 1 1 0 reflection.

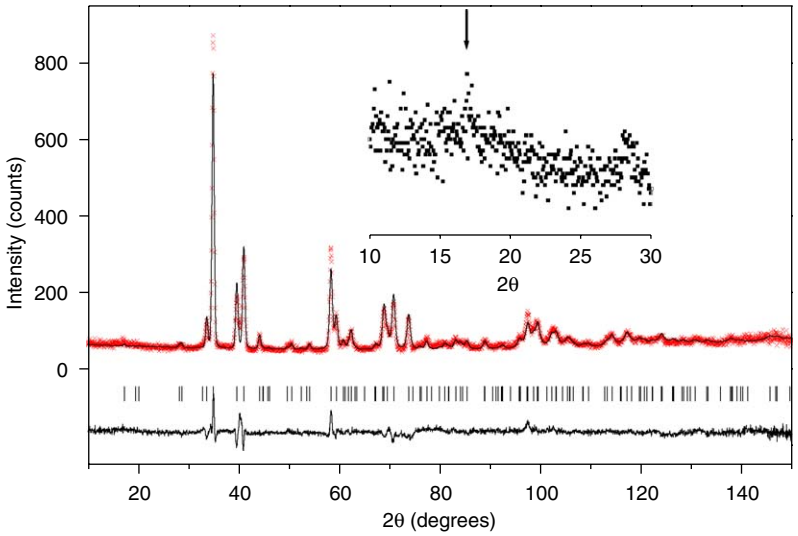

Fig. 2. Observed and calculated neutron profiles for the Rietveld refinement of Sr_2MnSbO_6. The format is the same as in Fig. 1.

octahedra demonstrating the correct space group to be $I4/m$. The structure was then refined in this space group. As anticipated from the weakness of the 1 0 1 reflection it was not possible to obtain a satisfactory fit to the observed data unless extensive anti-site disorder of the Mn^{3+} and Sb^{5+} cations was considered. The extent of this is estimated at around 40%. About 50% is a statistical distribution and would correspond to a fully disordered structure in $I4/mcm$. The width of the 1 0 1 reflection indicates that the coherent size of the ordered domains is very small, these were estimated to be ca. 20 Å using the Scherrer formula [17]. It may be possible to enhance the extent of ordering by annealing of the sample at low temperatures, although we have not attempted such studies. The final refined structural parameters are given in Table 1 and selected bond distances are reported in Table 2.

It must be stressed that the observation of the weak, broadened, superlattice reflections associated with the cation ordering relies on the use of high-resolution diffraction data. The reflections clearly observed in the high-resolution synchrotron data collected at the APS and shown in Fig. 1 are not observed using laboratory resolution data and indeed are just discernable using the lower resolution data obtained at the ANBF. We believe the failure of Lufaso et al. [7] to observe such reflections rests in their use of the lower resolution MRPD rather than the current HRPD at ANSTO's HIFAR reactor, the resolution of the HRPD being $\Delta d/d \approx 2 \times 10^{-3}$ whereas for the MRPD $\Delta d/d \approx 6 \times 10^{-3}$.

Table 1
Structural parameters for Sr_2MnSbO_6 at 25 °C, obtained from refinement using powder neutron diffraction data in space group $I4/m$ and at 900 °C in space group $Fm3m$

RT, space group $I4/m$, $a = 5.5313(4)$ Å, $c = 8.0832(7)$ Å					
Atom	R_p 6.90	R_{wp} 8.85	R_{exp} 4.81	GOF 3.39	R_{Bragg} 4.75
	x	y	z	Biso	N
Sr	0	0.5	0.25	1.19(9)	0.25
Sb/Mn	0	0	0	−1.84(19)	0.073(2)/0.052(2)
Mn/Sb	0	0	0.5	−1.84(19)	0.073(2)/0.052(2)
O1	0	0	0.2404(16)	0.84(5)	0.25
O2	0.7793(14)	0.7116(12)	0	0.84(5)	0.50
Temperature = 900 °C, space group $Fm3m$, $a = 7.9829(15)$ Å					
	R_p 7.65	R_{wp} 9.50	R_{exp} 5.96	GOF 2.54	R_{Bragg} 1.84
Sr	0.25	0.25	0.25	1.9(2)	0.04167
Sb/Mn	0	0	0	−1.3(1)	0.0132(2)/0.0076(2)
Mn/Sb	0.5	0.5	0.5	−1.3(1)	0.0132(2)/0.0076(2)
O1	0	0	0.2486(19)	2.7(1)	0.1250(0)

Table 2
Selected bond distances (Å) in Sr_2MnSbO_6

Bond	RT	900 °C
Sb–O1	1.943(13) × 2	2.007(15) × 6
Sb–O2	2.008(10) × 4	
	Avg. 1.986	
Mn–O1	2.098(13) × 2	1.984(15) × 6
Mn–O2	1.938(10) × 4	
	Avg. 1.991	

Neutron diffraction data for Sr_2MnSbO_6 were also collected at 900 °C. At this temperature the structure was cubic and the pattern was refined in $Fm\bar{3}m$, this choice allowing for rock-salt like ordering of the Mn^{3+} and Sb^{5+} cations. The refinement again indicated there was considerable anti-site disorder, this being estimated from the Rietveld refinements to be 37%. It appears that there is no thermally induced mixing of the two *B*-site cations at temperatures below 900 °C.

The structure at room temperature is characterized by partial cation ordering and octahedra tilting (Fig. 3). Both the Mn^{3+} and Sb^{5+} cations have a tetragonal distorted octahedral geometry with the Mn^{3+}-rich site having a two long and four short Mn–O geometry and the Sb^{5+}-rich site a two short and four long environment. The distortion of the MnO_6 octahedra is presumably driven by the JT effect, with a small contribution from the octahedra tilting. The space group symmetry then requires the second cation distort in the opposite sense—that is the axial bonds shorten and the equatorial bonds lengthen, this is illustrated in Fig. 3. This effect is seen in other ordered double perovskites such as Sr_2NiWO_6 where the WO_6 octahedra shows a small tetragonal elongation and the NiO_6 octahedra a tetragonal compression [20]. Nevertheless the magnitude of the distortion in the present case is noticeably larger, ca. 0.16 Å for the Mn–O bonds and 0.07 Å for the Sb–O bonds, than observed in Sr_2NiWO_6 where the difference between axial and equatorial bond lengths is ca. 0.01 Å. Thus it is apparent that the observed distortion of the SbO_6 octahedra is a consequence of the JT distortion of the MnO_6 octahedra. It would be interesting to establish using high-resolution diffraction methods if the closely related oxide Sr_2MnTaO_6 has a true random distribution of the Mn and Ta cations as reported by Lufaso et al. [7] or if it is, like Sr_2MnSbO_6 it is extensively disordered.

The cubic structure in $Fm\bar{3}m$ cannot accommodate a JT distortion of the MO_6 octahedra and for both cation sites the six M–O bond distances are required to be equal. The observed Mn–O and Sb–O distances are unexceptional. There is a small increase in the average Sb–O distance upon heating whereas the average Mn–O distance actually decreases slightly. It is possible that this decrease reflects the quenching of the JT effect however given the magnitude of the standard deviations in these distances further speculation on the cause of this is unwarranted.

Having established the structure of Sr_2MnSbO_6 in both the tetragonal and cubic phases we next investigated the temperature dependence of the structure. As shown in Fig. 4 increasing the temperature results in a progressive reduction of the tetragonal distortion so that above 550 °C the material is cubic.

The nature of the transition can be established by examination of the temperature dependence of a suitable order parameter [21]. Although the tilting of the octahedra is the obvious choice for the $I4/m$ to $Fm\bar{3}m$ ($a^0a^0c^-$ to

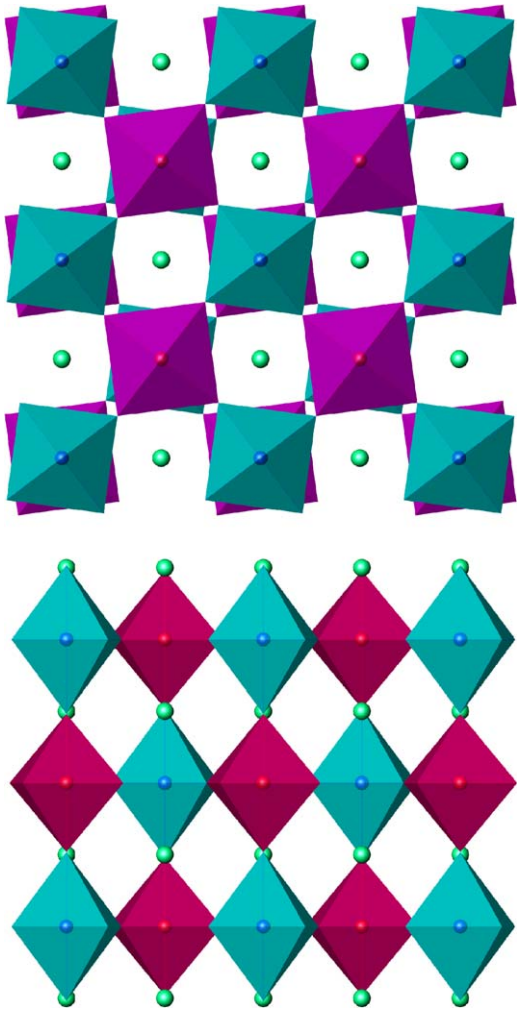

Fig. 3. Crystal structure of the tetragonal $I4/m$ structure of Sr_2MnSbO_6 in the 0 0 1 and 1 0 0 planes. The 0 0 1 view illustrates the effect of tilting of the octahedra and the 1 0 0 view highlights the alternate elongation and compression of the Mn/Sb octahedra. The Mn-rich sites are represented by the blue polyhedra.

$a^0a^0a^0$) transition, the insensitivity of the X-ray data to small displacements of the oxygen anions limits the precision with which this can be estimated. The variation of the X-ray lattice parameters (Fig. 3) provides an indication that whilst the transition is continuous it is not second order in nature. This is confirmed by analysis of the spontaneous strains. The tetragonal strain, e_t, is given by [22]

$$e_t = \frac{2}{\sqrt{3}}\left(\frac{c - a\sqrt{2}}{a_0}\right) \approx 2\sqrt{3}\left(\frac{c - a\sqrt{2}}{c + 2a\sqrt{2}}\right),$$

where c and a are the lattice parameters in the tetragonal phase, and a_0 is the extrapolated value of the lattice parameter from the observed expansion in the cubic structure. The plot of the temperature dependence of square of this strain, is linear (Fig. 5), demonstrating that the transition is continuous and tricritical in nature. Fitting of this curve indicates the transition temperature to be 521 °C.

Finally, it is worth considering why extensive disorder occurs in Sr_2MnSbO_6 whereas complete cation ordering is observed in the closely related JT system Sr_2CuWO_6, which is isostructural with Sr_2MnSbO_6 [8]. Firstly, we note that the CuO_6 octahedra shows a marked tetragonal elongation 2.283 vs. 1.938 Å and this is accompanied by a smaller tetragonal compression of the WO_6 group 1.914 vs. 1.943 Å. The compression of the WO_6 octahedra is a consequence of the JT-induced elongation of the CuO_6 octahedra. There are two significant differences between Sr_2MnSbO_6 and Sr_2CuWO_6, namely the difference in the size of the two B-site cations; with Δr_b being larger in the latter case, 0.045 Å compared to 0.13 Å, as is the charge difference. The oxides A_2CrNbO_6 $A = Ca^{2+}$ or Sr^{2+}, have similar sized cations on the B-site, $\Delta r_b = 0.025$ Å, and display extensive B-site cation disorder [23–25]. It appears that whilst charge and size effects induce cation ordering the size difference may be the most important. It is also worth noting that the larger size and smaller charge of Sb^{5+} cf. W^{6+} suggests this will be more polarizable and allow for more flexible geometries than W^{6+}, as seen by the very small distortion of the WO_6 octahedra in Sr_2CuWO_6.

Given a tetragonal distortion of the WO_6 octahedra is an unavoidable consequence of the JT distortion of the CuO_6 octahedra yet the size charge ratio of W^{6+} suggests such a distortion must be very small the next issue is how does the structure of Sr_2CuWO_6 respond to these two conflicting requirements. We suggest that this may be related to the magnitude of the BO_6 tilts, this being given by $\arctan \phi = 2(x_2 - y_2)$ where x_2 and y_2 are the fractional coordinates of the O(2) anion. The tilt is 9.0° in Sr_2CuWO_6, this having tolerance factor, t, of 0.972; $\phi = 7.0°$ and $t = 0.992$ in Sr_2MnSbO_6 and $\phi = 6.6°$, $t = 0.982$ in Sr_2NiWO_6. In the absence of any additional effects the tilt angle should increase as the tolerance factor decreases, these data show that the tilt angle in the double perovskites containing a JT active is larger than expected based purely on the geometric tolerance factor. A similar effect is observed in the two rutile-related halides $CaCl_2$ and $CrCl_2$ and is worthy of further study [26].

In conclusion we have demonstrated that the JT distortion of the $Mn^{III}O_6$ octahedra in the double perovskite Sr_2MnSbO_6 can be accommodated by a combination of tilting of the octahedra and concurrent distortion of the SbO_6 octahedra. We have found using high-resolution diffraction methods that cation ordering occurs in albeit within very small local domains. The absence of complete long range Mn:Sb ordering is rationalized in terms of the polarizibility of the Sb^{5+} cations and that this allows the oxide to adopt a distorted geometry. Even so the ordering requires considerable tilting of the MO_6 octahedra. Heating Sr_2MnSbO_6 results in a continuous transition to a cubic structure, in which the JT distortion of the Mn^{3+} cation is quenched. Analysis of

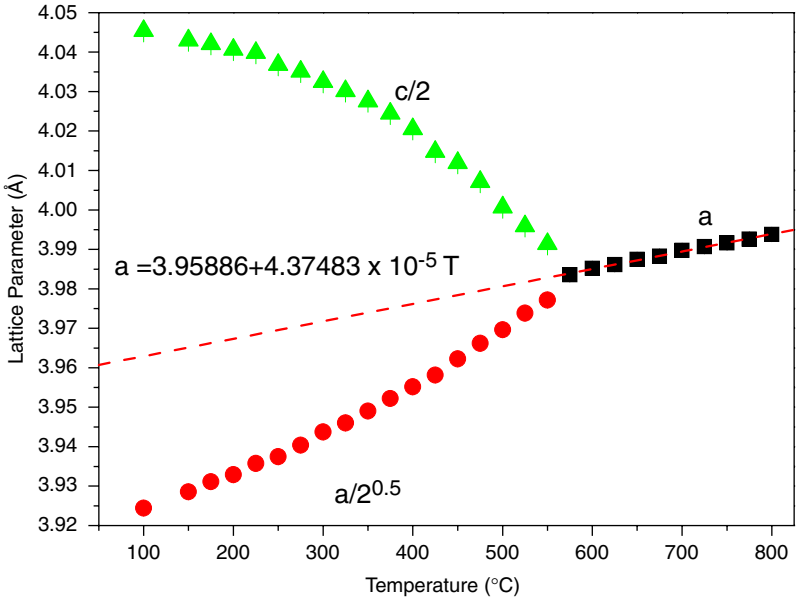

Fig. 4. Temperature dependence of the lattice parameters for Sr_2MnSbO_6 show the continuous transition to the cubic structure above 550 °C.

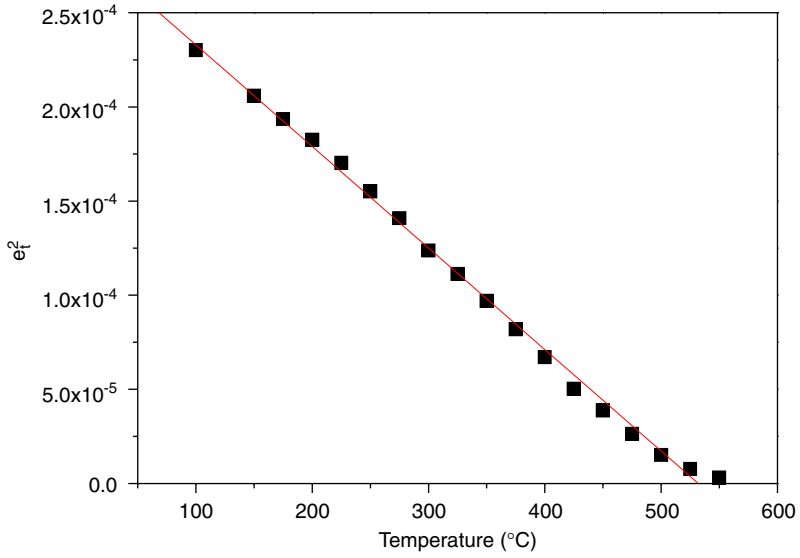

Fig. 5. Temperature dependence of the square of the spontaneous strain associated with the tetragonal distortion. The solid line is a linear fit and demonstrates the transition to be continuous and tricritical in nature.

the spontaneous strain shows this transition is tricritical, rather than second order in nature.

Acknowledgments

This work has been partially supported by the Australian Research Council. The synchrotron diffraction measurements were supported by the Australian Synchrotron Research Program, which is funded by the Commonwealth of Australia under the Major National Research Facilities program. The Australian Institute of Nuclear Science and Engineering supported the neutron diffraction experiments. The assistance of Drs. James Hester at the ANBF, Margaret Elcombe at ANSTO and Peter Lee at APS is gratefully acknowledged.

References

[1] C.J. Howard, H.T. Stokes, Acta Crystallogr. B 54 (1998) 782–789.
[2] R.H. Mitchell, Perovskites Modern and Ancient, Almaz Press Inc., Ontario, 2002.
[3] A.P. Ramirez, J. Phys.: Condens. Matter 9 (1997) 8171–8199.
[4] F. Sher, A. Venimadhav, M.G. Blamire, K. Kamenev, J.P. Attfield, Chem. Mater. 17 (2005) 176–180.
[5] Z. Fang, K. Terakura, J. Kanamori, Phys. Rev. B 63 (2001) 184408/1–184408/7.

[6] G.-L. Liu, J.-S. Zhou, J.B. Goodenough, Phys. Rev. B 64 (2001) 144414–144414/7.
[7] M.W. Lufaso, P.M. Woodward, J. Goldberger, J. Solid State Chem. 177 (2004) 1651–1659.
[8] D. Iwanaga, Y. Inaguma, M. Itoh, J. Solid State Chem. 147 (1999) 291–295.
[9] C.J. Howard, B.J. Kennedy, B.C. Chakoumakos, J. Phys: Condens. Matter 12 (2000) 349–365.
[10] M.A. Carpenter, C.J. Howard, B.J. Kennedy, K.S. Knight, Phys. Rev. B 72 (2005) 024118/1–024118/15.
[11] B.J. Kennedy, C.J. Howard, B.C. Chakoumakos, J. Phys.: Condens. Matter 11 (1999) 1479–1488.
[12] R.D. Shannon, Acta Crystallogr. A 32 (1976) 751–767.
[13] G. Blasse, J. Inorg. Nucl. Chem. 27 (1965) 993–1003.
[14] S.C. Abrahams, Acta Crystallogr. B 52 (1996) 790–805.
[15] T.M. Sabine, B.J. Kennedy, R.F. Garrett, G.J. Foran, D.J. Cookson, J. Appl. Crystallogr. 28 (1995) 513–517.
[16] C.J. Howard, C.J. Ball, R.L. Davis, M.M. Elcombe, Aust. J. Phys. 36 (1983) 507–518.
[17] B. A. Hunter, C.J. Howard, Rietica for Windows, 1.7.7, Sydney, 1997.
[18] C.J. Howard, B.J. Kennedy, P.M. Woodward, Acta Crystallogr. B 59 (2003) 463–471.
[19] H. Boysen, Z. Kristallogr. 220 (2005) 726.
[20] Q. Zhou, B.J. Kennedy, C.J. Howard, M.M. Elcombe, A.J. Studer, Chem. Mater. (2005).
[21] J.-C. Tolédano, P. Tolédano, The Landau Theory of Phase Transitions, World Scientific Publishing, Singapore, 1987.
[22] M.A. Carpenter, Strain and Elasticity at Structural Phase Transitions in Minerals, The Mineralogical Society of America, Washington, DC, 2000.
[23] M. Cheah, B.J. Kennedy, unpublished work.
[24] J.-H. Choy, J.-H. Park, S.-T. Hong, D.-K. Kim, J. Solid State Chem. 111 (1994) 370–379.
[25] J.-H. Choy, S.-T. Hong, K.-S. Choi, J. Chem. Soc. Faraday Trans. 92 (1996) 1051–1059.
[26] C.J. Howard, B.J. Kennedy, C. Curfs, Phys. Rev. B 72 (2005) 214114.